Predicting jet ignitability using a PDF transport model

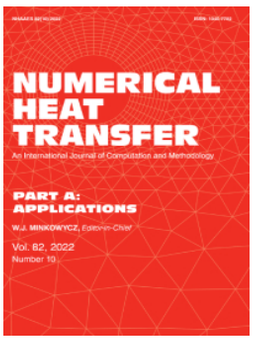

Taylor & Francis
Taylor & Francis Group

Numerical Heat Transfer, Part A: Applications
An International Journal of Computation and Methodology

ISSN: (Print) (Online) Journal homepage: https://www.tandfonline.com/loi/unht20

Predicting jet ignitability using a PDF transport model

Peter S. Cumber

To cite this article: Peter S. Cumber (2022) Predicting jet ignitability using a PDF transport model, Numerical Heat Transfer, Part A: Applications, 82:10, 601-618, DOI: 10.1080/10407782.2022.2083436

To link to this article: https://doi.org/10.1080/10407782.2022.2083436

Published online: 16 Jun 2022.

NUMERICAL HEAT TRANSFER, PART A: APPLICATIONS
2022, VOL. 82, NO. 10, 601–618
https://doi.org/10.1080/10407782.2022.2083436

Predicting jet ignitability using a PDF transport model

Peter S. Cumber

School of Engineering and Physical Sciences, Heriot-Watt University, Edinburgh, Scotland, UK

ABSTRACT

For the first time the probability of ignition is calculated successfully using a PDF transport model. At present the model is only accurate where jet intermittency effects are small, away from the jet boundary. A conclusion of this investigation is the probability of ignition field is sensitive to the micro-mixing model used. In this article, four micro-mixing models are implemented and the modified Curl model demonstrated to be the most accurate for the jet ignitability experiments simulated.

ARTICLE HISTORY
Received 27 November 2021
Accepted 13 May 2022

KEYWORDS
Composition PDF transport; jet ignitability; micro-mixing model; Monte-Carlo method

1. Introduction

When assessing the accidental release of a flammable gas the potential for a turbulent jet to ignite and light back to form a rim-stabilized or lifted free jet flame must be evaluated. Previous work [1], has shown that the static flammability limits are a poor indication of a turbulent jet's ignitability characteristics as ignition is observed when the mean concentration is below the static lower flammability limit (LFL). This occurs due to the fluctuating nature of a turbulent flow such that although the mean concentration is below the LFL for some of the time the instantaneous fuel concentration is between the flammability limits.

This phenomenon is investigated experimentally by a number of groups [1–3]. The first paper on jet ignitability is Birch et al. [1], where the instantaneous volume fraction in a methane jet is measured using laser Raman spectroscopy. From the instantaneous concentration field the probability density function (PDF) is constructed [4]. Once the PDF is available the probability of ignition can be evaluated.

$$\mathrm{P}_i = \int_{LFL}^{UFL} P(c)dc \tag{1}$$

In subsequent papers [2, 3], the ignitability of free turbulent jets for natural gas, propane and a simulated town gas are investigated using a spark ignition system. In [3], the probability of ignition and the conditional light back probability are measured. When sparking a flammable jet, the ignition probability is the number of times combustion local to the sparking device is observed compared to the total number of sparks. The conditional light back probability is determined by the number of local combustion events that ultimately propagate upstream to the source to form a stable flame relative to the total number of ignition events. Schefer et al. [5], investigated jet ignitability in hydrogen jets using a non-intrusive laser ignition source.

CONTACT Peter S. Cumber p.s.cumber@hw.ac.uk School of Engineering and Physical Sciences, Heriot-Watt University, Riccarton Campus, Scotland, Edinburgh, EH14 4AS, UK.

Nomenclature

C_1,C_2	turbulence model parameters
C_φ ,κ	constants in the micro-mixing models
C_μ	turbulence model parameter
d	source diameter
f_i	particles representing the PDF
$\tilde{f}$	mean mixture fraction
$\tilde{f}''^2$	variance of mixture fraction
F_f	flammability factor
Fr	Froude number
g	gravitational acceleration
g'	reduced gravity
k	turbulence kinetic energy
l_t	turbulent length scale
N_i	number of ignition events
N_m	number of pairs of mixing particles in the modified Curl model
N_r	number of control volumes in the radial direction
N_{sam}	number of particles per control volume
N_{trial}	number of sparking events
P	probability density function
P_i	probability of ignition
P_k	production of turbulence kinetic energy
r	radial coordinate
r_0	source radius
Re	Reynolds number
U_0	source velocity
U	axial velocity component
V	radial velocity component
z	axial coordinate

Greek Symbols

Δr	mesh spacing in the radial direction
Δt^*	pseudo time-step
Δz	space step in the z coordinate direction
ε	dissipation rate of turbulence kinetic energy
κ	Von Karman constant
μ_{eff}	effective dynamic viscosity
ρ	density
σ_k	turbulent Prandtl number for turbulence kinetic energy
σ_ε	turbulent Prandtl number for dissipation rate of turbulence kinetic energy
σ_i	probability of ignition uncertainty
σ_P	turbulent Prandtl number for the PDF transport equation
ω	turbulent frequency

Subscript

amb	ambient value
i	ignition property
t	turbulence property
0	source conditions

Over bar

$\bar{}$	Reynolds average
$\tilde{}$	Favre average

The development of jet ignitability models is limited. Birch and coworkers [1–3], constructed the flammability factor,

$$\mathrm{F}_f = \int_{LFL}^{UFL} P_{APX}\left(\tilde{c}, \widetilde{c''^2}; c\right) dc$$

where P_{APX} is a prescribed approximate PDF with mean and variance, $\tilde{c}$, $\widetilde{c''^2}$ that is a combination of a Gaussian profile and an intermittency factor. The mean concentration and its variance are taken from the measured data. Gant et al. [6], extended the flammability factor model using a variety of empirical correlations, rather than measured mean concentration and concentration variance. Gant et al.'s model is a true model in the sense that other than source conditions no more information from the experiment is required, however as one might expect it is no better than Birch's model when applied to the measurements of Smith et al. [3].

Alvani and Fairweather [7], extended the jet ignitability model of Birch et al. [1], by proposing a three part prescribed PDF weighted by the proportion of time the flow is fully turbulent, intermittent or in the viscous super layer [8]. Alvani and Fairweather [7], accept that in the form presented the composite PDF model is likely not to apply universally, but for the turbulent flows considered [2, 9, 10], good agreement between experiment and theory is demonstrated. Alvani and Fairweather [7], used measured mean concentration and variances to predict PDFs as well as the prescribed PDF in combination with a parabolic flow model. The mixture fraction and mixture fraction variance are calculated by solving modeled transport equations. Alvani and

Fairweather [11], extended the previous model [7], by implementing a transport equation for the intermittency factor [12], in combination with the parabolic flow model. Alvani and Fairweather [11], use two different approaches to model turbulence, a k-ε turbulence model [13], and a Reynolds stress transport model [14], however results are inconclusive with respect to which turbulence model is the most accurate in this context.

With the advancement of the PDF transport model it is possible to calculate the PDF as a function of location without prescribing the generic shape of the PDF. The original motivation for investigating the PDF transport model is that it treats turbulence-chemistry interaction exactly [15]. The PDF transport model is applied to many combustion phenomena [16–18].

There is also much interest in PDF transport modeling for turbulence-radiation interaction (TRI) [19, 20]. This is because the PDF transport model is often solved using a Monte-Carlo method where the PDF is represented as a collection of particles. In the context of TRI each particle represents the instantaneous conditions within a control volume. This lends itself to a stochastic simulation of TRI [21–23].

The final application of the PDF transport model is the one considered here, the simulation of non-reacting jets where the evaluation of the PDF is of interest. There is little work in this field. As already stated turbulence-chemistry interaction is treated exactly in the PDF transport model, however a number of other terms require some form of approximation, such as the treatment of molecular mixing. Molecular mixing is represented in the PDF transport equation by a micro-mixing model. Wouters et al. [24], were one of the first groups to simulate non-reacting turbulent jets using a PDF transport model. They implemented four micro-mixing models and simulated a number of neutrally buoyant jets investigated experimentally by Dowling and Dimotakis [25]. Some interesting results are presented in [24], but issues with sampling size make it difficult to differentiate between the different micro-mixing models predictive capability.

More recently Cumber [26, 27], applied a composition PDF transport model to the natural gas jet of Birch et al. [28], using the Curl model [29], modified Curl (MC) model [30], interaction by exchange with the mean (IEM) model [31], a variant of the Langevin model [27], and the Euclidean minimum spanning tree (EMST) model [32]. Birch et al. [28], natural gas (95% methane) jet is used in Cumber [26, 27], for validation purposes as a wide range of measured data exist characterizing the jet, such as the PDF, mean mixture fraction, mixture fraction variance, as well as higher mixture fraction moments such as the skewness and kurtosis. From Cumber [26, 27], it is clear that the mean mixture fraction and mixture fraction variance predicted fields are insensitive to the micro-mixing model implemented. For higher mixture fraction moments and the PDF there is sensitivity to the micro-mixing model implemented with the MC model and a variant of the Langevin model being more accurate than the IEM model and the EMST model in this application.

In this article the composition PDF model in combination with a parabolic flow model is applied to the jet ignitability measurements of Birch et al. [1, 2] and Smith et al. [3].

2. Mathematical model

The mathematical model for simulating ignition characteristics for turbulent jets is presented below.

2.1. Parabolic flow equations

The Reynolds Averaged Navier Stokes (RANS) equations describe the conservation of mass and momentum in an axisymmetric frame of reference and are the basis of the flow model enabling the prediction of the velocity field. The thin shear layer approximation is applied and the assumption that the pressure field is approximately constant is used to simplify the system of transport equations and the solution methodology. These approximations change the nature of the system to be a parabolic system, with the axial coordinate taking on a time like quality. This enables a

marching scheme to be implemented, starting at the source and the flow fields computed downstream of the source.

$$\frac{\partial(\overline{\rho}\widetilde{U})}{\partial z}+\frac{1}{r}\frac{\partial(r\overline{\rho}\widetilde{V})}{\partial r}=0$$

$$\overline{\rho}\widetilde{U}\frac{\partial\widetilde{U}}{\partial z}+\overline{\rho}\widetilde{V}\frac{\partial\widetilde{U}}{\partial r}=\frac{1}{r}\frac{\partial}{\partial r}\left(r\ \mu_{eff}\frac{\partial\widetilde{U}}{\partial r}\right)+g(\overline{\rho}-\rho_{amb})$$

The basis of the solution algorithm is the GENMIX code [33]. The turbulent viscosity is calculated using the k-ε turbulence model [13], modified to account for the plane jet/round jet anomaly [34]. The correction for the simulation of turbulent round jets is that originally proposed by Morse [35].

$$\frac{\partial(\overline{\rho}\widetilde{U}k)}{\partial z}+\frac{1}{r}\frac{\partial(r\overline{\rho}\widetilde{V}k)}{\partial r}=\frac{1}{r}\frac{\partial}{\partial r}\left(r\frac{\mu_{eff}}{\sigma_k}\frac{\partial k}{\partial r}\right)+\overline{\rho}(P_k-\epsilon)$$

$$\frac{\partial(\overline{\rho}\widetilde{U}\epsilon)}{\partial z}+\frac{1}{r}\frac{\partial(r\overline{\rho}\widetilde{V}\epsilon)}{\partial r}=\frac{1}{r}\frac{\partial}{\partial r}\left(r\frac{\mu_{eff}}{\sigma_k}\frac{\partial\epsilon}{\partial r}\right)+\overline{\rho}\frac{\varepsilon}{k}(C_1P_k-C_2\epsilon)$$

$$P_k=\mu_{eff}\left(\frac{\partial\widetilde{U}}{\partial r}\right)^2\quad\mu_{eff}=\mu_l+\frac{C_\mu\ \overline{\rho}\ k^2}{\epsilon}$$

$$C_1=1.4-3.4\left(\frac{k}{\varepsilon}\frac{d\widetilde{U}}{dz}\right)_{cl}^3$$

$$C_m=0.09, C_2=1.84, \sigma_k=1\ \text{and}\ \sigma_e=1.3$$

2.2. PDF transport model

The composition PDF transport model for a non-reacting flow can be stated in Cartesian coordinates as [19],

$$\frac{\partial\rho P}{\partial t}+\frac{\partial\widetilde{U}_i\rho P}{\partial x_i}=-\frac{\partial}{\partial x_i}\left\{\langle u_i''|\psi\rangle\ \rho P\right\}+\frac{\partial}{\partial\psi}\left\{\left\langle\frac{1}{\rho}\frac{\partial J_i}{\partial x_i}\middle|\psi\right\rangle\rho P\right\}\tag{2}$$

where ψ represents the instantaneous mixture fraction space and P is the probability density such that,

$$\mathrm{P}(\psi)\mathrm{d}\psi=\text{Probability}\{\psi\le f\le\psi+d\psi\}$$

The angled brackets in (2) represent conditional averages. In (2) the terms on the left are exact and those on the right require modeling. The two modeled terms represent turbulent convection in physical space and molecular mixing in scalar space respectively. The turbulent convection is modeled typically using a gradient diffusion assumption. The molecular mixing term is replaced by a micro-mixing model where there is choice over the approach taken.

In an axisymmetric frame of reference with the gradient diffusion term included the PDF transport model reads,

$$\overline{\rho}\widetilde{U}\frac{\partial P}{\partial z}+\overline{\rho}\widetilde{V}\frac{\partial P}{\partial r}=\frac{1}{r}\frac{\partial}{\partial r}\left(r\frac{\mu_{eff}}{\sigma_P}\frac{\partial P}{\partial r}\right)+\left(\frac{dP}{dt}\right)_{mm}\tag{3}$$

2.2.1. Micro-mixing models

Any micro-mixing model must ideally satisfy a number of constraints or properties as listed below [36].

I. The mean concentration is unchanged by the micro-mixing model.
II. For an inert homogeneous flow, the concentration variance should decay over time.
III. The concentration should remain in the allowable space.
IV. Mixing should be local in composition space.
V. In a homogeneous turbulent field, the concentration PDF should relax to a Gaussian profile.

At present no micro-mixing model satisfies all of the above properties. A discussion of the respective strengths and weaknesses of the micro-mixing models considered here is given in [36]. Four micro-mixing models are implemented the IEM model, the MC model, the EMST model and the limited Langevin model. In this article each micro-mixing model is given a brief description only. The interested reader should consult the references cited. The IEM model,

$$\frac{df_i}{dt} = -\frac{1}{2} C_\varphi \omega \left(f_i - \widetilde{f}\right) \tag{4}$$

is one of the more popular micro-mixing models as it is straight forward to implement and for inhomogeneous flows for the most part gives reasonably accurate results. $C_\varphi \omega > \dot{\varphi}/\sigma \upsilon \beta >$ is a parameter in the model that can take a value between 0.5 and 4 with an accepted value of 2 being optimal for most flows, ω is the turbulent frequency,

$$\omega = \frac{\epsilon}{k}$$

The Curl model [29], is derived on the basis that molecular mixing can be represented by the interaction of droplets that coalesce and disperse.

$$\left(\frac{dP}{dt}\right)_{mm} = 2C_\varphi \omega \int P\left(f + f'\right) P\left(f - f'\right) df - \omega P(f) \tag{5}$$

The above model, (5) is computationally costly if implemented as part of a finite volume method to solve (2) [36], whereas it is straight forward using a Monte-Carlo method. As part of a Monte-Carlo method, the molecular mixing process is represented at each time-step and for each control volume by,

$$\mathrm{N}_m = \frac{3}{2} C_\varphi \omega \ \mathrm{N}_{sam} \Delta \mathrm{t}$$

pseudo random pairs of particles being chosen to form two new "averaged" particles.

$$f_i^{new} = f_i + \frac{1}{2}\alpha\left(f_j - f_i\right)$$

$$f_j^{new} = f_j + \frac{1}{2}\alpha\left(f_i - f_j\right)$$

where α is a pseudo random variable in the unit interval.

The third model, EMST is a particle interaction model based on a mapping closure model where particles are separated into an active and non-activate set. Only the active particles can mix and they mix on the basis of how close they are in composition space, determined by constructing a binary tree with each particle being a leaf on the tree. Particles move between the two sets as the solution evolves, see [32, 37, 38] for more details.

The final micro-mixing model included in the study is the Langevin model. This can be thought of as an extension of the IEM model with an additional stochastic term introduced originally to model Brownian motion. In its discrete form the evolution of a particle is given as,

$$f_i^{n+1} = f_i^n - \frac{1}{2}(C_\varphi + \kappa)\omega \ \Delta t \ \left(f_i^n - \widetilde{f}\right) + \sqrt{\kappa \ \omega \ \Delta t \widetilde{f''}^2} z_G \tag{6}$$

Table 1. Summary of jet source conditions.

Ref.	d/mm	U_0/ms^{-1}	Fuel	Re	Fr
Birch [1, 2, 28]	12.65	21.2	Natural Gas	16000	91
Smith [3]	6.35	50	Natural gas	21750	301
Smith [3]	6.35	20	Propane	29200	108
Smith [3]	6.35	55	Town gas*	12950	432

*Hydrogen = 50%, natural Gas = 30%, and nitrogen = 20%.

Where κ is an additional constant typically assigned a value in the range 0.3 to 2.1, Δt is the time-step and z_G is a pseudo-random variable satisfying a Gaussian distribution with zero mean and unit variance. This model suffers from a serious weakness when the concentration field is bounded as is the case for mixture fraction; the Gaussian random variable implies that it is possible to calculate particle trajectories that are outside the physically acceptable region. A number of extensions to the Langevin model have been proposed to address this problem. One of these is the binomial Langevin model [39]. As part of this investigation the version of the binomial Langevin model implemented in this study is that proposed by Wouters et al. [24], however the model did not perform well, with poor accuracy and long run-times. In its place a simple limiter function is placed on the mixture fraction particles to prevent excursion outside of the unit interval. This notionally violates property *I* but [27], showed that in reality this is not a serious problem. This version of the Langevin model is labeled "L Langevin" in the figures below.

2.2.2. Monte-Carlo method

The numerical method used to solve (3) is the same as that presented in Pope [15]. It is repeated here for convenience. The starting point for the numerical solution algorithm is the representation of a PDF in any control volume as a collection of particles.

$$\{f_i(r,z)\}_{i=1}^{N_{sam}}$$

The transport equation is Discretized and solved using a fractional step method [15],

$$P(r,z+\Delta z) = (I+\Delta t^* M)(I-\Delta t^* V)(I+\Delta t^* D)P(r,z) + O\left(\Delta t^{*2},\ \Delta r\right) \tag{7}$$

$$\Delta t^* = \frac{\Delta z}{\widetilde{U}(r,z)}$$

The operations applied in sequence above represent the diffusion, advection and mixing of particles to produce the new PDF at location, $(r,\ z+\Delta z)$, represented by the new set of particles.

$$\{f_i(r,z+\Delta z)\}_{i=1}^{N_{sam}}$$

These three processes impose upper bounds on the pseudo-time step, Δt^* to ensure a stable solution. Therefore, the pseudo time-step is prescribed to be,

$$\Delta t^*_{PDF} = \min\{0.9\ min\{\Delta t_D,\ \Delta t_A,\ \Delta t_M\},\ \Delta t^*\}$$

where the three time steps, Δt_D, Δt_A, and Δt_M, are upper limits defined by the stability conditions for the respective processes. Note for the micro-mixing step Δt_M can be infinite depending on the model used. The solution of the PDF transport equation continues until the axial space step Δz is reached.

The particles in the samples, f_i represent the instantaneous mixture fraction. Any mean property that is a function of mixture fraction can be calculated as a sample average. For example, the mean density is given as,

$$\overline{\rho} = \frac{1}{N_{sam}} \sum_{i=1}^{N_{sam}} \rho(f_i)$$

where the instantaneous density is a weighted harmonic mean of the fuel and air density.

Given the PDF the probability of ignition can be evaluated from (1) or by counting the particles within the flammability limits compared to the total number of particles in a control volume.

3. Jet ignitability studies

In this article a number of free turbulent jets are used for validating the ignition model. The sources for data and turbulent jet conditions are summarized in Table 1. For convenience each jet will be referred to by its Reynolds number.

For all jets the source of flammable gas issues from a pipe of fifty diameters length such that at the exit plane the flow is well approximated to be fully developed pipe flow. In Birch [28] the instantaneous concentration field is measured using a laser Raman spectroscopy system. The source pipe is mounted on a three dimensional traverse operated by lead screws with a positional accuracy of ±0.1 mm. Birch et al.'s [28]. experimental set-up is a turbulent free natural gas (95% methane) jet with a Reynolds number of 16,000. The gas enters the jet through a tube with a diameter of 12.65 mm. The velocity profile at the source is typical of fully developed turbulent pipe flow with a mean axial source velocity of 21.2 m/s.

For the ignitability studies the ignition system comprises of two 320 mm long electrodes with a separation distance of 50 mm. The ends of the electrodes have a curved profile such that the spark gap is 3 mm. The electrodes are positioned in the flow such that they have a vertical orientation. The influence of the electrodes on the flow is small as confirmed using the Schlieren method [3]. A spark energy in excess of 100 mJ is produced by an inductive spark generator. For all fuels over the range of the flammable concentration this is above the minimum ignition energy. For each location of the spark generator the probability of ignition is measured as,

$$\mathrm{P}_i = \frac{N_i}{N_{trial}}$$

where for a set of N_{trial} spark events the number of successful ignitions, N_i is noted. For these experiments the standard deviation of the statistical uncertainty of P_i is,

$$\sigma_i = \sqrt{\frac{P_i(1-P_i)}{N_{trial}}}$$

For an ignition probability of 0.5, 400 trials give a standard deviation of 0.025. As P_i moves away from 0.5 the absolute uncertainty decreases, however for low probability of ignition the relative uncertainty can be large. More details of the experimental configuration can be found in [1–3, 28].

4. Numerical details and boundary conditions

The boundary conditions imposed at the jet source are consistent with that of fully developed pipe flow. The axial velocity profile is a 1/7 power law. The turbulence properties are calculated by assuming turbulence is isotropic and in equilibrium. The turbulence kinetic energy is prescribed such that the turbulence velocity is 5% of the mean flow.

$$k_0 = (0.05U_{0,cl})^2$$

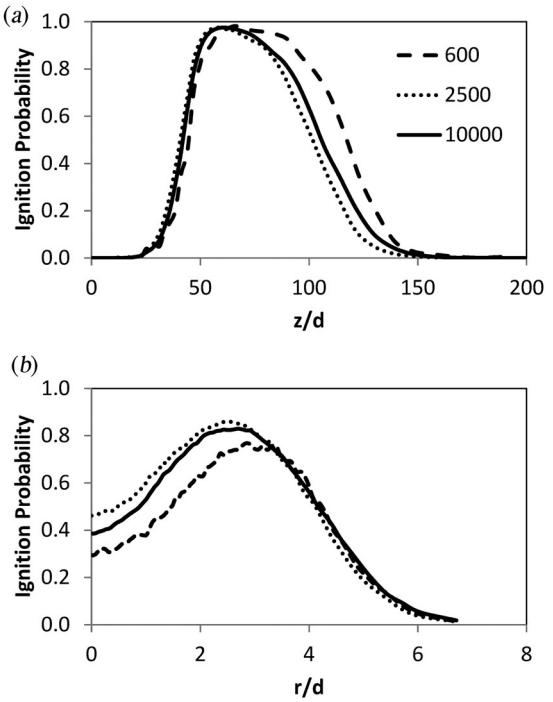

Figure 1. The predicted ignition probability using three different sample sizes: (a) $r/d = 0$ and (b) $z/d = 40$.

$$\epsilon_0 = \frac{k_0^{1.5}}{l_t}$$

$$l_t = \min\{\kappa\ (r_0 - r), 0.1 r_0\} \Big/ C_\mu^{0.75}$$

At the source the concentration is all flammable gas and all particles are set to unity. At the edge of the jet the concentration field is 100% air and the particles defining the PDF are given a value of zero.

The finite volume mesh at the source spans the radius of the tube, with a symmetry boundary imposed on the jet axis. Downstream of the source the finite volume mesh expands as the jet spreads radially, due to turbulent mixing and the entrainment of the surrounding air.

The numerical error in the solution of the parabolic flow model is controlled by the number of control volumes in the radial coordinate direction, N_r and the fractional step size in the axial coordinate direction. The fractional step and the number of control volumes in the radial direction are linked so simulations using a given mesh will be referred to by N_r, the number of control volumes in the radial direction alone. To determine the appropriate value for N_r a number of simulations are completed where N_r is systematically doubled and the fractional step halved until the predicted flow fields do not change significantly. For the turbulent jets considered a value of N_r=80 yielded predicted flow fields insensitive to further refinement of the mesh as the difference in predicted mean mixture fraction is less than 5% when N_r is increased to 160. A mesh sensitivity study is presented in some detail in previous publications [40–42] so will not be repeated here.

Similarly, the error in the solution to the composition PDF transport model is governed by the statistical error in the Monte-Carlo simulation and is investigated in a similar way to the sensitivity to the mesh. For a fixed finite volume mesh two simulations are calculated using a sample of N_{sam}=600 and N_{sam} =2500 particles per control volume. The solutions are compared and if the

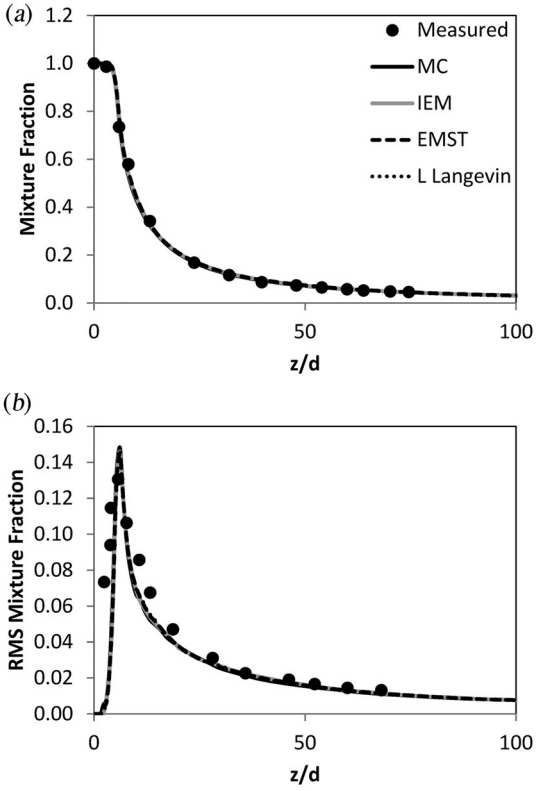

Figure 2. Comparison of the measured and predicted axial distribution for the $Re = 16000$ natural gas jet, $r/d = 0$, of (a) mean mixture fraction and (b) RMS mixture fraction.

differences in the two simulations are significant then a simulation with N_{sam}=10000 particles is calculated. This process is continued until the change in the predicted mean mixture fraction and mixture fraction moments do not change, to the resolution of the figures presented below. A detailed study investigating the sensitivity of the predicted fields to the sample size is presented in [27]. It will not be repeated here, suffice it to say that N_{sam}=10000 gives predicted mean mixture fraction and higher mixture fraction moments that are free from significant statistical error.

The one aspect of the sensitivity of prediction to N_r and N_{sam} that has not been considered previously is the predicted ignition probability. For the $Re = 16000$ natural gas jet the predicted ignition probability for N_r=80 on the axis and radially at $z/d = 40$ is shown in Figure 1. For both distributions three curves are shown calculated with N_{sam}=600, 2500 and 10000. Simulations with N_{sam}=40000 were also completed to confirm that to the resolution of the figure the predicted ignition probability is insensitive to increasing the sample size beyond N_{sam}=10000.

The run-time and computer storage requirements of the PDF transport model for non-reacting jets are investigated in some detail in Cumber [26, 27]. The computer storage and computer run-time requirements for the simulation of non-reacting jets using the PDF transport model scale linearly with the number of particles. The computer run-time depends weakly on the micro-mixing model implemented with the modified Curl model, IEM model and EMST model having similar run-times for the same number of particles with the limited Langevin model simulations requiring more run-time.

All of the simulations presented in this article are calculated on a standard PC with an Intel® Core™ i5-2400 CPU@ 3.1 GHz processor. To give an indication of the computer run-time required to complete a simulation using the PDF transport model implemented with the modified

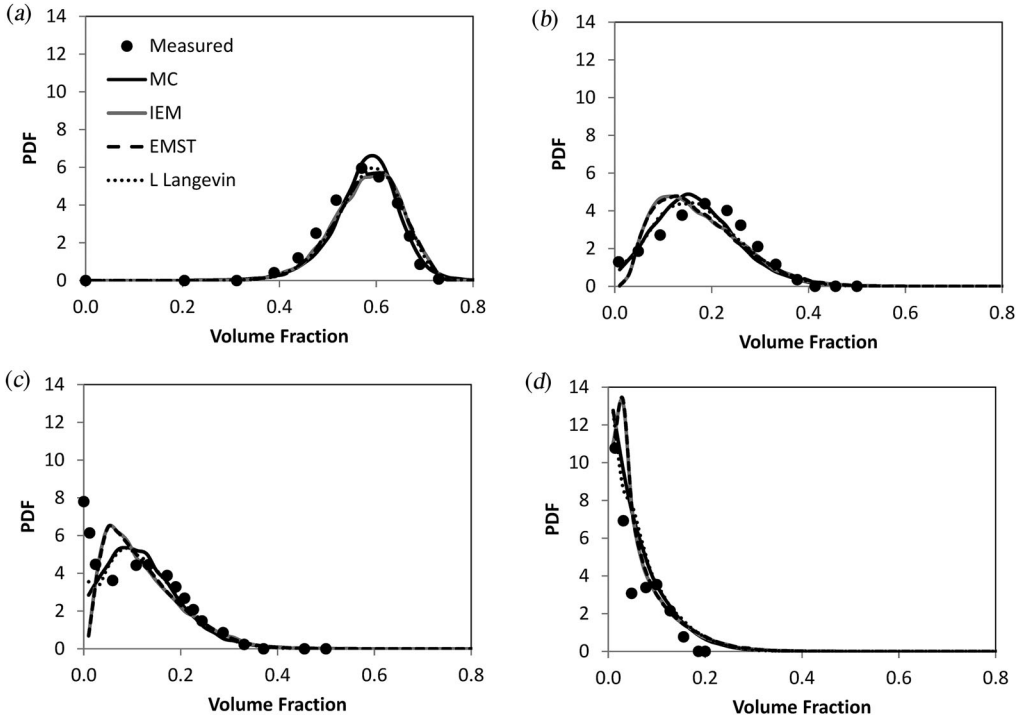

Figure 3. Comparison of the measured and predicted PDF for the $Re = 16000$ natural gas jet at $z/d = 10$, (a) $r/d = 0$, (b) $r/d = 1.3$, (c) $r/d = 1.49$, and (d) $r/d = 1.8$.

Curl micro-mixing model, Birch et al.'s natural gas jet [28], is simulated with N_r=80 and z_{last}=200d, using N_{sam}=10000 particles requires fifteen minutes to complete.

5. Validation study

In this section the utility of the model for predicting ignition probabilities is explored. This is done in two stages. Firstly, the models ability to predict the structure of turbulent non-reacting jets is demonstrated followed by a comparison of predicted and measured ignitability characteristics for a number of turbulent jets.

5.1. Jet structure

A detailed validation of the composite model, i.e., the parabolic flow model in combination with the PDF transport model is given in [27]. Here a subset of the validation study is presented. Figure 2*a* shows a comparison of the predicted and measured mean mixture fraction for $r/d = 0$. In the figure there are four predicted curves, calculated using the micro-mixing models discussed in section 2.2.1. The four predicted curves are almost identical and all agree well with the measured distribution. In Figure 2*b* the measured and predicted RMS mixture fraction on the axis is shown and similar to the mean mixture fraction all four micro-mixing model predictions are indistinguishable and in close agreement with the measured distribution. For example, the predicted peak in the RMS mixture fraction is 0.15 located at $z/d = 6.1$ compared to a measured peak of 0.13 located at $z/d = 5.7$.

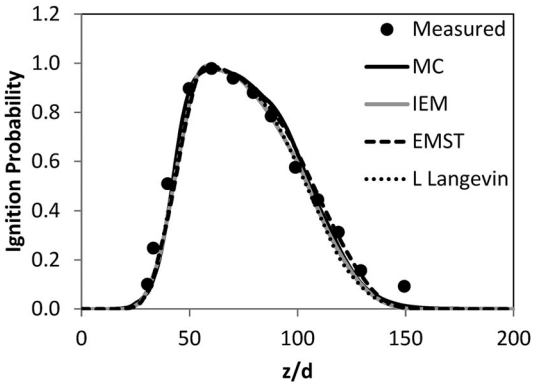

Figure 4. Comparison of the measured and predicted ignition probability for the $Re = 16000$ natural gas jet, $r/d = 0$.

A superficial and incorrect conclusion from Figure 2 is the turbulent jet structure for non-reacting jets is insensitive to the micro-mixing model implemented. For higher mixture fraction moments the predicted distributions are different for different micro-mixing models [27].

The importance of the micro-mixing model to the prediction of the jet structure is demonstrated in Figure 3 where the predicted and measured PDF are compared at four locations, $z/d = 10$, $r/d = 0$, 1.3, 1.49 and 1.8. The predicted PDFs are calculated with 50000 particles separated into 50 equi-spaced intervals spanning the unit interval. The measured and predicted PDFs on the jet axis are shown in Figure 3*a*. All four predicted curves can be distinguished but all are in close agreement with the measured PDF. In Figure 3*b* and 3*c* the concentration PDF located at $r/d = 1.3$ and $r/d = 1.49$ are shown respectively. The predicted PDF curves can be grouped into two sets. The modified Curl model and the limited Langevin model produce very similar predicted PDFs that for the most part are in agreement with the measured PDF except there is a tendency for the peak of the predicted PDF to be located at a smaller value of instantaneous volume fraction than the measured PDF. A further deficiency is the measured PDF at $r/d = 1.49$ has a spike located at the origin. This is not reproduced by any of the micro-mixing models as the spike is a consequence of jet intermittency and the model as it stands takes no account of jet intermittency [11].

Considering the IEM model and EMST model predictions of the PDFs at $r/d = 1.3$ and 1.49, these models produce the same predicted PDF distributions and they are inferior to the modified Curl model and the limited Langevin model. It is difficult to determine what aspect of these models makes them poor candidates for predicting the PDF distribution here. In [27] all four micro-mixing models are applied to the DNS of scalar mixing in homogeneous turbulence [43]. For this scenario similar behavior is exhibited in that the IEM model and the EMST model give qualitatively poor predictions of the PDF of the scalars evolution in time, compared to the performance of the modified Curl model or the limited Langevin model. The reason for the IEM models poor performance at reproducing the evolution of the scalar PDF is it does not satisfy Property *V*, however given that the jet is not homogeneous it is difficult to see how this is a factor.

The final location where the measured PDF is reported, at $r/d = 1.8$ is included for completeness but jet intermittency effects dominate ad it is not possible to comment on the micro-mixing models' performance.

5.2. Jet ignitability

Considering the probability of ignition of the $Re = 16000$ jet [1, 2], Figure 4 shows a comparison of the measured and predicted probability of ignition on the jet axis, $r/d = 0$. The measured

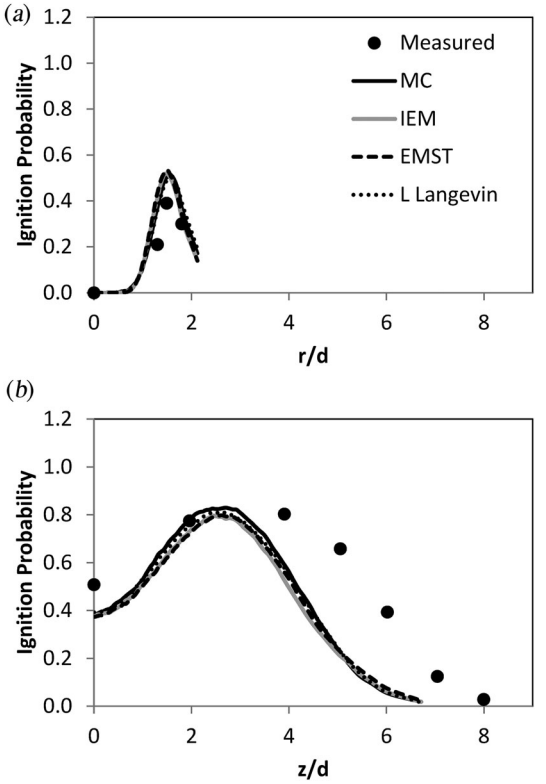

Figure 5. Comparison of the measured and predicted ignition probability for the $Re = 16000$ natural gas jet (a) $z/d = 10$ and (b) $z/d = 40$.

ignition probability is calculated using the spark ignition methodology described in Section 3. Four predicted probability of ignition curves are shown in Figure 4 each representing the probability of ignition calculated using a different micro-mixing model. Note in all figures where the predicted probability of ignition is compared with the measured distribution, four curves are shown. Returning to Figure 4 the different predicted curves are in close agreement with each other but unlike the mean mixture fraction distributions different curves can be distinguished. Overall the level of agreement between the model predictions and the measured data is very good. The location of the measured initial rise in probability of ignition at $z/d = 30$ is reproduced by the model. Further downstream the measured peak in ignition probability is present in the predicted distributions. The model also predicts the slow decline in ignition probability downstream of the peak value as well as the more rapid decrease in measured ignition probability for $z/d > 100$. The one possible weakness in the predicted ignition probability is the under prediction of the measured distribution at $z/d = 150$. It is unclear why this occurs but it could be to do with the sample size as 400 spark events might not be sufficient to give an accurate estimate of the ignition probability when it approaches zero [1, 2]. This point is revisited below.

Further measured probability of ignition data for the $Re = 16000$ turbulent jet is available for model validation. The radial distributions of the probability of ignition at $z/d = 10$ and $z/d = 40$ are available for comparison with equivalent predicted curves. At $z/d = 10$ the measured probability of ignition is evaluated by integrating the PDF between the flammability limits. A comparison of the measured and predicted probability of ignition at $z/d = 10$ is given in Figure 5*a*. There is insufficient measured data to determine a measured distribution but the comparison of the predicted curves with the measurements is encouraging. Similar to Figure 4 it is possible to distinguish different predicted curves calculated with different micro-mixing models, but they are very

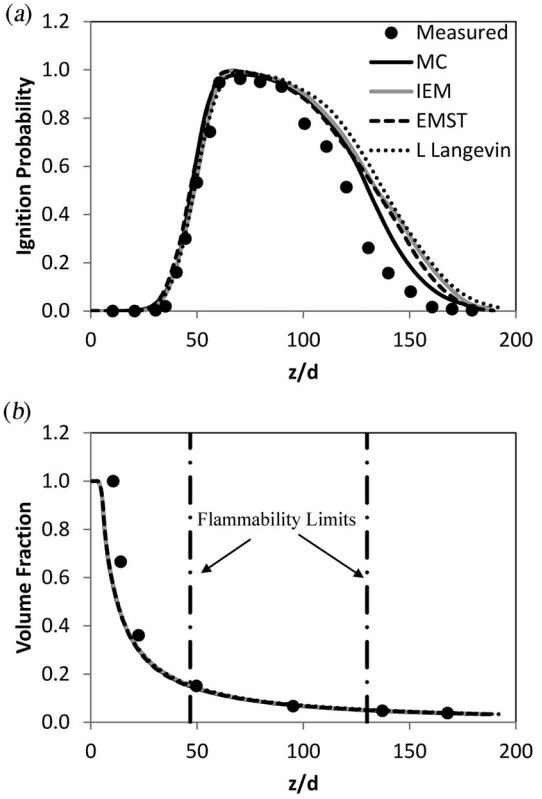

Figure 6. Comparison of the measured and predicted axial distribution for the $Re = 21750$ natural gas jet, $r/d = 0$, of (a) ignition probability and (b) volume fraction.

similar. Further downstream at $z/d = 40$ the predicted probability of ignition under predicts the measured distribution, particularly near the jet edge, $r/d > 5$. This is likely to be due to the model not including jet intermittency effects [11].

Note the $Re = 16000$ turbulent jet is the most comprehensive data set for validation purposes as the jet structure is characterized accurately as well as the probability of ignition is measured on the axis and radially at two downstream locations. For the remaining jet ignitability data sets used in the validation study only the mean concentration distribution and probability of ignition on the jet axis are available.

The last natural gas jet ignitability experiment in the validation study is reported by Smith et al. [3] and is $Re = 21750$. In this experiment the source diameter and velocity are 6.35 mm and 50 m/s respectively. The measured and predicted probability of ignition is shown in Figure 6*a*. From the figure it is clear that all four predicted ignition probabilities agree well with the location of rapid increase in the measured probability of ignition, $z/d = 40$. Further downstream the predicted curves spread out with the modified Curl micro-mixing model being closer to the measured profile than the other three micro-mixing models. In Figure 6*b* the volume fraction distribution on the axis, $r/d = 0$ is shown. All four model predictions of the volume fraction to the resolution of the figure are the same. Comparing the model prediction with the measured volume fraction distribution the agreement in the far field, for $z/d > 50$ is excellent. In the near field the predicted volume fraction is below the measured volume fraction. The static flammability limits for methane are indicated on the figure to allow comparison with the probability of ignition distribution. As expected the static flammability limits are good indicators for the location of the P_i=0.5, consistent with the turbulent nature of the jet.

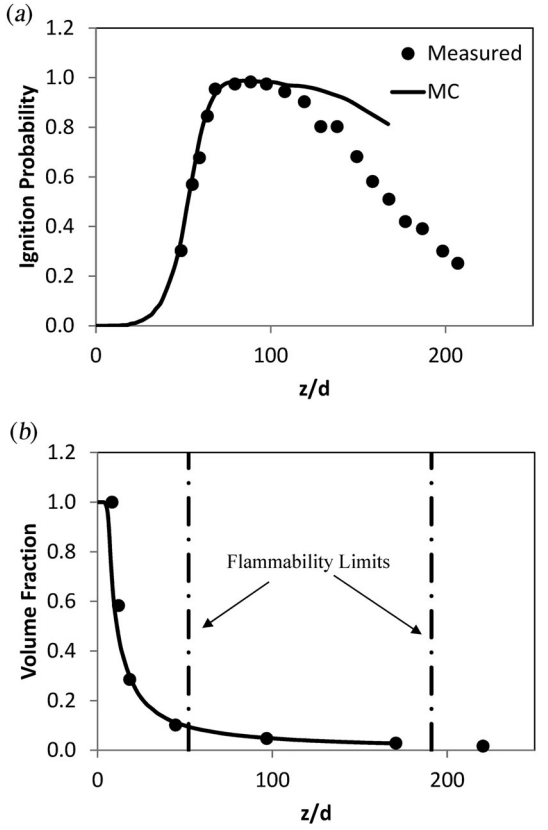

Figure 7. Comparison of the measured and predicted axial distribution for the $Re = 29200$ propane jet, $r/d = 0$, of (a) ignition probability and (b) volume fraction.

The penultimate jet ignitability experiment in the validation study is $Re = 29200$. This is a turbulent propane jet with a source diameter and velocity of 6.35 mm and U_0=20 m/s respectively. As can be seen in Figure 7, the simulation of a dense turbulent jet with a relatively low Froude number,

$$Fr = \frac{U_0}{\sqrt{g'd}} = 108$$

has a dramatic effect on the predicted jet structure and probability of ignition field. In Figure 7*a* only one predicted curve for the probability of ignition is given. The predicted probability of ignition curve is calculated using the modified Curl model. Only one prediction is shown as all other micro-mixing models failed to complete the simulation at a short downstream distance from the source. The modified Curl simulation failed at $z/d = 170$. Upstream of $z/d = 170$ the modified Curl prediction of ignition probability is disappointing, the initial rise in the measured probability of ignition is reproduced but from $z/d = 120$ the predicted probability of ignition is remote from the measured distribution. Figure 7*b* shows a comparison of the measured and predicted volume fraction on the axis, $r/d = 0$. Where the predicted volume fraction distribution is calculated the predicted curve is in close agreement with the measured data. For example, at $z/d = 97$ the measured volume fraction is 0.048 compared to a predicted value of 0.05. Similar to Figure 6*b*, the static flammability limits are indicated on Figure 7*b*. For $z/d > 170$ the lower flammability limit is calculated by linear interpolation on the measured data.

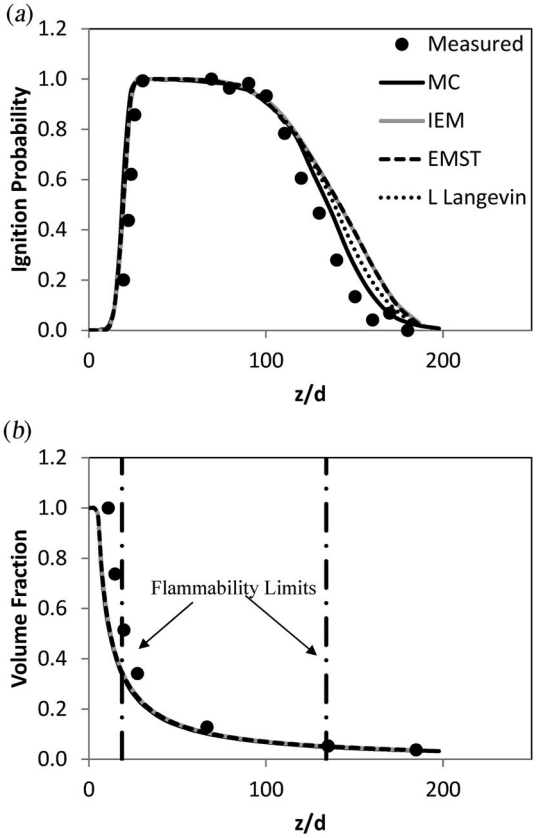

Figure 8. Comparison of the measured and predicted axial distribution for the $Re = 12500$ town gas jet, $r/d = 0$, of (a) ignition probability and (b) volume fraction.

The breakdown of the model for this jet is due to the jet having a relatively low Froude number meaning that the transition from a high momentum jet to a plume occurs close to the source compared to a high Froude number jet. A further difficulty is that the high density of propane compared to air means that the turbulent jet not only transitions to a plume but will also ultimately stall. The parabolic approximation in the flow model is only valid for flows exhibiting jet like behavior. As the turbulent jet spreads out the parabolic assumption weakens until the flow can no longer be modeled in this way. The dense nature of propane means that this problem occurs much closer to the source due to it creating a sink term in the RANS equations due to the body force. Note that the first jet considered also has a low Froude number, $Fr = 91$, however in this case the buoyancy of the natural gas provides a source of momentum, moving the transition to a buoyant plume further downstream. Revisiting Figure 6*a* the poor performance of the model for the ignition probability at $z/d = 150$ could be due to the validity of the parabolic flow model being compromised.

The final jet ignitability experiment is $Re = 12950$. The fuel is simulated town gas with a composition of 50% by volume hydrogen, 30% natural gas and 20% nitrogen. Figure 8*a* shows the measured and predicted ignition probability. The results are similar to the natural gas ignitability experiment, $Re = 21750$, see Figure 6*a*. The four micro-mixing models produce different predictive curves all having the same shape and agreeing well with the measured ignition probability for $z/d < 100$. Further downstream the modified Curl model prediction is in closest agreement with the measured ignition probability distribution. For example, at $z/d = 130$ the measured probability of ignition is P_i=0.47 compared to a predicted value calculated using the modified Curl model of

P_i=0.57 and the EMST model prediction of P_i=0.64, the model with the poorest accuracy. In Figure 8*b* the measured and predicted volume fraction on the axis of the town gas jet is shown together with the static flammability limits for town gas. In the near field the measured volume fraction is underpredicted by the composite model, but further downstream the model agreement with the measured data is acceptable. Given all four micro-mixing models predict the same mean volume fraction distribution it seems likely that the prescription of turbulent mixing may be the cause of the poor agreement in the near field, but without further information it is difficult to take this argument forward.

6. Conclusion

In this article, a PDF transport model is used to simulate a number of jet ignitability experiments. Where the parabolic flow model is valid the model is demonstrated to predict the probability of ignition on the jet axis with reasonable accuracy. Four micro-mixing models are implemented in the PDF transport model; the modified Curl model, the IEM model, the EMST model and a variant of the Langevin model. The predicted probability of ignition is sensitive to the micro-mixing model used unlike the mean mixture fraction field and the RMS mixture fraction field. Of the four micro-mixing models the modified Curl model is the most accurate.

There is limited measured ignitability data away from the jet axis. Near the edge of the jet for the limited data available the composite model tends to underpredict the measured ignitability data as in this regime jet intermittency is important and at present the model takes no account of this effect.

There are a number of ways forward to improve the model that could be potentially fruitful. Jet intermittency could be included in a similar way to Alvani and Fairweather [11], making it possible to predict ignitability at the edge of the jet. It should be noted that for calculating hazard contours the ignition probability on the jet axis is sufficient as it gives the maximum distance to a given ignition probability. Another possibility for improving the model would be to extend its capability to predict jet light-back probability as at present no theoretical model exists for this phenomenon. It may be possible to calculate the jet light-back probability with some degree of accuracy based on the ignition probability and turbulent burning velocity using a stochastic approach.

References

[1] A. D. Birch, D. R. Brown, M. G. Dodson and J. R. Thomas, "Studies of flammability in turbulent flows using laser Raman spectroscopy, 17th Symp (Int) on combustion," *Combust. Inst.*, vol. 17, no. 1, pp. 307–314, 1979. DOI: 10.1016/S0082-0784(79)80032-6.

[2] A. D. Birch, D. R. Brown and M. G. Dodson, "Ignition probabilities in turbulent flows 18th Symp (Int) on combustion,", *Combust Inst.*, vol. 18, no. 1, pp. 1775–1780, 1981. DOI: 10.1016/S0082-0784(81)80182-8.

[3] M. T. E. Smith, A. D. Birch, D. R. Brown and M. Fairweather, "Studies of ignition and flame propagation in turbulent jets of natural gas, propane and a gas with a high hydrogen content 21st Symp (Int) on combustion," *Combust Inst.*, vol. 21, no. 1, pp. 1403–1408, 1988. DOI: 10.1016/S0082-0784(88)80372-2.

[4] H. Chen, S. Chen and R. H. Kraichnan, "Probability distribution of a stochastically advected scalar field," *Phys Rev Lett.*, vol. 63, no. 24, pp. 2657–2660, 1989. DOI: 10.1103/PhysRevLett.63.2657.

[5] R. W. Schefer, G. H. Evans, J. Zhang, A. J. Ruggles and R. Greil, "Ignitability limits for combustion of unintended hydrogen releases: experimental and theoretical results," *Int J Hydrogen Energy.*, vol. 36, no. 3, pp. 2426–2435, 2011. DOI: 10.1016/j.ijhydene.2010.04.004.

[6] S. E. Gant, M. R. Pursell, C. J. Lea, A. M. Thyer and S. Connolly, "Flammability of hydrocarbon/CO_2 mixtures: Part 2 Predictive models for gas jet ignition," *IChemE SY P. Series*, vol. 156, pp. 456–467, 2011.

[7] R. F. Alvani and M. Fairweather, "Ignition characteristics of turbulent jet flows," *Trans IChemE Part A.*, vol. 80, no. 8, pp. 917–923, 2002. DOI: 10.1205/026387602321143471.

[8] E. Effelsberg and N. Peters, "A composite model for the conserved scalar pdf," *Combust Flame.*, vol. 50, pp. 351–360, 1983. DOI: 10.1016/0010-2180(83)90075-5.

[9] J. C. LaRue and P. A. Libby, "Temperature fluctuations in the plane turbulent wake," *Phys. Fluids.*, vol. 17, no. 11, pp. 1956–1967, 1974. DOI: 10.1063/1.1694651.

[10] R. W. Schefer and R. W. Dibble, "Mixture fraction field in a turbulent non-reacting propane jet," *AIAA.*, vol. 39, no. 1, pp. 64–72, 2001. DOI: 10.2514/3.14698.

[11] R. F. Alvani and M. Fairweather, "Prediction of the ignition characteristics of flammable jets using intermittency-based turbulence models and a prescribed pdf approach," *Comput. Chem Eng.*, vol. 32, no. 3, pp. 371–381, 2008. DOI: 10.1016/j.compchemeng.2007.02.007.

[12] D. A. Olivieri, M. Fairweather and S. Falle, "Rans modelling of intermittent turbulent flows using adaptive mesh refinement methods," *J Turbulence.*, vol. 11, pp. 1–18, 2010.

[13] W. P. Jones and B. E. Launder, "The prediction of laminarization with a two equation model of turbulence," *Int. J Heat Mass Transfer.*, vol. 15, no. 2, pp. 301–314, 1972. DOI: 10.1016/0017-9310(72)90076-2.

[14] W. R. Jones and P. Musonge, "Closure of the Reynolds stress and scalar flux equations," *Phys. Fluids.*, vol. 31, no. 12, pp. 3589–3604, 1988. DOI: 10.1063/1.866876.

[15] S. B. Pope, "A Monte Carlo method for the PDF equations of turbulent reactive flow," *Comb Sci Tech.*, vol. 25, no. 5-6, pp. 159–174, 1981. DOI: 10.1080/00102208108547500.

[16] J. Janicka and N. Peters, "Prediction of turbulent jet diffusion flame lift-off using a PDF transport equation, 19th Symp (Int) on combustion," *Combustion Inst.*, vol. 19, no. 1, pp. 367–374, 1982. DOI: 10.1016/S0082-0784(82)80208-7.

[17] R. R. Cao, S. B. Pope and A. R. Masri, "Turbulent lifted flames in a vitiated coflow investigated using joint PDF calculations," *Comb Flame.*, vol. 142, no. 4, pp. 438–453, 2005. DOI: 10.1016/j.combustflame.2005.04.005.

[18] R. P. Lindstedt, V. D. Milosavljevic and M. Perron, "Turbulent burning velocity predictions using transported PDF methods, 33rd Symp (Int) on Combustion," *Combustion Inst.*, vol. 33, no. 1, pp. 1277–1284, 2011. DOI: 10.1016/j.proci.2010.05.092.

[19] G. Li and M. F. Modest, "Application of composition PDF methods in the investigation of turbulence-radiation interactions," *J. Quant Spec Radiat Transf.*, vol. 73, no. 2–5, pp. 461–472, 2002. DOI: 10.1016/S0022-4073(01)00218-7.

[20] S. Mazumder and M. F. Modest, "A PDF approach to modelling turbulence-radiation interactions in nonluminous flames," *Int J. Heat Mass Transfer.*, vol. 42, no. 6, pp. 971–991, 1999. DOI: 10.1016/S0017-9310(98)00225-7.

[21] P. S. Cumber and O. Onokpe, "Turbulent radiation interaction in jet flames: sensitivity to the PDF," *Int J. Heat Mass Transfer.*, vol. 57, no. 1, pp. 250–264, 2013. DOI: 10.1016/j.ijheatmasstransfer.2012.10.032.

[22] P. S. Cumber, "Efficient modelling of turbulence-radiation interaction in hydrogen jet flames," *Numer. Heat Transf. Part B.*, vol. 63, no. 2, pp. 85–114, 2013. DOI: 10.1080/10407790.2013.740395.

[23] P. S. Cumber, "Validation study of a turbulence radiation interaction model: Weak, intermediate and strong TRI in jet flames," *Int J Heat Mass Transfer.*, vol. 79, pp. 1034–1047, 2014. DOI: 10.1016/j.ijheatmasstransfer.2014.08.073.

[24] H. A. Wouters, P. A. Nooren, T. W. J. Peeters and D. Roekaerts, "Effects of micro-mixing in gas-phase turbulent jets," *Int J Heat Fluid Flow.*, vol. 19, no. 2, pp. 201–207, 1998. DOI: 10.1016/S0142-727X(97)10025-X.

[25] D. R. Dowling and P. E. Dimotakis, "Similarity of the concentration field of gas-phase turbulent jets," *J. Fluid Mech.*, vol. 218, no. 1, pp. 109–141, 1990. DOI: 10.1017/S0022112090000945.

[26] P. S. Cumber, "Application of the PDF transport model to non-reacting jets using an adaptive Monte-Carlo method," *Numer. Heat Transf. Part B.*, vol. 70, no. 2, pp. 91–110, 2016.

[27] P. S. Cumber, "Micro-mixing model performance for non-reacting flows using a consistent Monte-Carlo method," *Numer. Heat Transf. Part B.*, vol. 70, no. 2, pp. 517–536, 2016.

[28] A. D. Birch, D. R. Brown, M. G. Dodson and J. R. Thomas, "The turbulent concentration field of a methane jet," *J. Fluid Mech.*, vol. 88, no. 3, pp. 431–449, 1978. DOI: 10.1017/S0022112078002190.

[29] R. L. Curl, "Dispersed phase mixing: 1 theory and effects in simple reactors," *AIChE J.*, vol. 9, no. 2, pp. 175–181, 1963. DOI: 10.1002/aic.690090207.

[30] C. Dopazo, "Probability density function approach for a turbulent axisymmetric heated jet. Centreline evolution," *Phys. Fluids.*, vol. 18, no. 4, pp. 397–181, 1975. DOI: 10.1063/1.861163.

[31] J. Janicka, W. Kolbe and W. Kollmann, "Closure of the transport equation for the probability density function of turbulent scalar fields," *J Non-Equilib. Thermodynam.*, vol. 4, pp. 47–66, 1979.

[32] S. Subramaniam and S. B. Pope, "A mixing model for turbulent reactive flows based on a Euclidean minimum spanning trees," *Comb Flame*, vol. 115, no. 4, pp. 487–514, 1998. DOI: 10.1016/S0010-2180(98)00023-6.

[33] D. B. Spalding, *GENMIX: A General Computer Program for Two-Dimensional Parabolic Phenomena*, Oxford: Pergamon Press, 1977.

[34] S. B. Pope, "An explanation of the turbulent round-jet/plane-jet anomaly," *AIAA J.*, vol. 16, no. 3, pp. 279–281, 1978. DOI: 10.2514/3.7521.
[35] J. B. Moss, C. D. Stewart and K. Syed, "Flow field modelling of soot formation at elevated pressure, 22nd (Int) on combustion," *Combustion Inst.*, vol. 22, no. 1, pp. 413–423, 1989. DOI: 10.1016/S0082-0784(89)80048-7.
[36] D. C. Haworth, "Progress in probability density function methods for turbulent reacting flows," *Progress Energy Combus Sci.*, vol. 36, no. 2, pp. 168–259, 2010. DOI: 10.1016/j.pecs.2009.09.003.
[37] Z. Ren and S. B. Pope, "An investigation of the performance of turbulent mixing models," *Comb Flame*, vol. 136, no. 1–2, pp. 208–216, 2004. DOI: 10.1016/j.combustflame.2003.09.014.
[38] Z. Ren, S. Subramaniam and S. B. Pope, "Implementation of the EMST mixing model," 2002. http://tcg.mae.cornell.edu/emst.
[39] L. Valino and C. Dopazo, "A binomial Langevin model for turbulent mixing," *Physics Fluids A*, vol. 3, no. 12, pp. 3034–3037, 1991. DOI: 10.1063/1.857847.
[40] P. S. Cumber and M. Spearpoint, "Modelling lifted methane jet fires using the boundary layer equations," *Num Heat Transf. Part B, Fundament.*, vol. 49, no. 3, pp. 239–258, 2006. DOI: 10.1080/10407790500291921.
[41] O. Onokpe and P. S. Cumber, "Predicting the mean and RMS fields in subsonic hydrogen jet fires," *Fire Safety J.*, vol. 49, pp. 22–34, 2012. DOI: 10.1016/j.firesaf.2011.12.014.
[42] P. S. Cumber and M. Spearpoint, "A computational flame length methodology for propane jet fires," *Fire Safety J.*, vol. 41, no. 3, pp. 215–228, 2006. DOI: 10.1016/j.firesaf.2006.01.003.
[43] V. Eswaran and S. B. Pope, "Direct numerical simulations of the turbulent mixing of a passive scalar," *Phys. Fluids.*, vol. 31, no. 3, pp. 506–520, 1988. DOI: 10.1063/1.866832.